

Short Communication

Guided waves group and energy velocities via finite elements

M.N. Ichchou*, S. Akrouf, J.-M. Mencik

Laboratoire de Tribologie et Dynamique des Systèmes, École Centrale de Lyon - 36, Avenue Guy de Collongue, 69134 Ecully Cedex, France

Received 12 February 2007; received in revised form 30 April 2007; accepted 1 May 2007

Available online 29 June 2007

Abstract

In this note numerical sensitivity of a wave finite element approach and its post processing for group velocities and energy velocities estimation is dealt with. Precisely, aliasing effects is discussed first. Calculation of guided waves group velocity through a numerical procedure is given. A wave track versus frequencies criteria is employed. Energetics of multi-mode guided wave propagation is also discussed. Analytical expressions of energy velocities are provided. Energy velocities are compared to group velocities, and the sensitivity of energy velocities to the finite element system characteristics is discussed.

© 2007 Published by Elsevier Ltd.

1. Introduction

Calculations of guided wave energy and group velocities in complex waveguides is the main concern of this communication. In a recent paper [1] a numerical approach was offered in order to extract dispersion curves for guided uniform structures. The proposed approach was implemented in a finite element code and enables numerical extraction of guided wavenumbers and deformed shape characteristics. A similar approach was very recently studied by Mace [2], whilst Finnveden [3] extended a spectral finite-element-like approach for wavenumber estimation in complex homogeneous and uniform waveguides.

The present note completes the above-mentioned paper [1] and addresses two questions:

- Numerical sensitivity of the approach and aliasing.
- Calculation of guided waves group velocity (through a numerical procedure) and energy velocity (through guided structure energetics).

The numerical sensitivity of the propagation features is covered first in this note. Then the study focusses on the definition of the geometrical characteristics of the modeled structures. Here, the purpose is to fix, for a given propagation length, the highest wavenumber to be extracted. Aliasing effects connected to this question support our choice and offer some rules to be considered for a safe use of the approach.

*Corresponding author. Equipe Dynamique des Systèmes et des Structures, Laboratoire de Mécanique des Solides, Génie Mécanique et Génie civil, 36 Avenue Guy de Collongue, BP 163, École Centrale de Lyon, 69134 Ecully Cedex, France.

Tel.: +33 4 72 18 62 30; fax: +33 4 72 18 91 44.

E-mail address: mohamed.ichchou@ec-lyon.fr (M.N. Ichchou).

Energy and group velocities of such complex guided waves are thus analyzed. Group velocities are extracted through a finite difference calculation associated with a necessary numerical classification criterion for a wave track purposes. The proposed criterion is based upon symplectic properties of the spectral problem. It allows propagating branches to be rigorously identified as frequency increases. Calculated group velocities are then compared with estimations of energy velocities. The latter requires energy flow and stored energy densities to be expressed. Some of our results extend the work offered in Refs. [4,5] among others. Some numerical experiments are then presented to complete the discussion.

2. Brief outline of the formulation

2.1. Finite element wave propagation in a straight structure

The dynamics of straight elastic and dissipative structures is studied. A sample straight structure is illustrated in Fig. 1: in the present framework, the system is assimilated to a set of identical subsystems, connected along the principal direction, say axis x , and whose left and right cross-sections (x -axis description) are denoted as L and R , respectively. The length of each subsystem, along axis x , is denoted as d . The formulation is based on the finite element model of a typical subsystem, as illustrated in Fig. 1, and whose kinematic variables, displacements and forces, are written as \mathbf{q} and forces \mathbf{F} , respectively. Mesh compatibility at coupling interfaces between subsystems is assumed, implying that the left and right cross-sections of the given subsystem contains the same number of degrees of freedom, say n . The dynamic equilibrium equation of this subsystem, at frequency $\omega/2\pi$, can be stated as follows [6]:

$$\begin{bmatrix} \mathbf{D}_{LL} & \mathbf{D}_{LR} \\ \mathbf{D}_{RL} & \mathbf{D}_{RR} \end{bmatrix} \begin{bmatrix} \mathbf{q}_L \\ \mathbf{q}_R \end{bmatrix} = \begin{bmatrix} \mathbf{F}_L \\ \mathbf{F}_R \end{bmatrix}, \tag{1}$$

where $(n \times n)$ matrix $\mathbf{D}_{ij} = \mathbf{K}_{ij} - \omega^2 \mathbf{M}_{ij}$ ($\{i, j\} \in \{L, R\}$) stands for the ij component of the dynamic stiffness operator condensed on the left and right cross-sections, namely \mathbf{D} [6]. Here, \mathbf{K} and \mathbf{M} stand for the stiffness and mass matrices, respectively. Dissipation can be considered through standard FEM models. According to Bloch’s theorem [7], the dynamics of the global waveguide can be expanded on specific wave solutions of the form

$$\mathbf{q}_R = \mu \mathbf{q}_L \tag{2}$$

and

$$\mathbf{F}_R = -\mu \mathbf{F}_L, \tag{3}$$

where μ denotes the propagation coefficient. Expressions (2) and (3) lead to an eigenvalue problem. Indeed, inserting Eqs. (2) and (3) into Eq. (1) leads to the following spectral problem [1]:

$$(\mathbf{D}_{RL} + \mu_i(\mathbf{D}_{LL} + \mathbf{D}_{RR}) + \mu_i^2 \mathbf{D}_{LR})(\Phi_{\mathbf{q}})_i = 0, \tag{4}$$

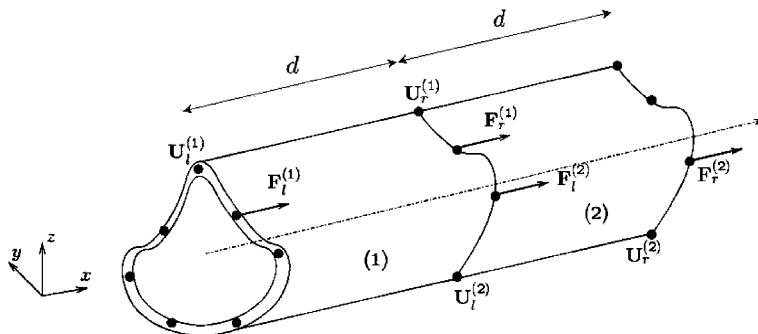


Fig. 1. Typical thin walled structure.

where $\{(\mu_i, (\Phi_Q)_i)\}_{i=1,\dots,2n}$ stands for the wave modes of the global system. A modified and well-conditioned format of the spectral problem can also be obtained. For this purpose, the use of a state vector representation is an interesting alternative to the spectral analysis which must be performed in the context of the numerical dispersion curve extraction (see Refs. [6,8] for detailed discussions). Indeed, given the following matrices:

$$S = \begin{bmatrix} -D_{LR}^{-1} D_{LL} & -D_{LR}^{-1} \\ D_{RL} - D_{RR} D_{LR}^{-1} D_{LL} & -D_{RR} D_{LR}^{-1} \end{bmatrix} \tag{5}$$

and matrix J , defined by

$$J = \begin{bmatrix} 0 & I \\ -I & 0 \end{bmatrix}, \tag{6}$$

it can be readily shown that:

$$S^T J S = J \tag{7}$$

meaning that S is symplectic [6]. Ultimately, a spectral problem can be established as

$$J \Phi_i = \mu_i S^T J \Phi_i, \tag{8}$$

which leads to

$$J^{-1} S^{-T} J \Phi_i = \mu_i \Phi_i, \tag{9}$$

and thus, considering that matrix S is symplectic ($S^{-T} = J S J^{-1}$ [6]),

$$S \Phi_i = \mu_i \Phi_i. \tag{10}$$

Here $\Phi_i = ((\Phi_Q)_i^T (\Phi_F)_i^T)^T$ stands for the i th eigenvector of operator S , which is decomposed into $(n \times 1)$ displacements q and forces F wave components. The frequency response of the global system can be expressed by expanding the kinematic variables of the considered subsystem on the basis of eigenvectors (see for instance Ref. [9]):

$$\begin{pmatrix} q_L \\ -F_L \end{pmatrix} = \begin{bmatrix} \Phi_Q \\ \Phi_F \end{bmatrix} Q_L \quad \text{and} \quad \begin{pmatrix} q_R \\ F_R \end{pmatrix} = \begin{bmatrix} \Phi_Q \\ \Phi_F \end{bmatrix} Q_R, \tag{11}$$

where Φ_Q and Φ_F stand for the matrices of eigenvectors $\{(\Phi_Q)_i\}_i$ and $\{(\Phi_F)_i\}_i$, respectively [9], and where Q_L and Q_R stand for the $(2n \times 1)$ generalized coordinates evaluated for the left and right boundaries of the subsystem, respectively. It has been shown in Refs. [10,11] that generalized coordinates Q_L and Q_R can be related in this way

$$Q_R = \begin{bmatrix} \mu & 0 \\ 0 & \mu^{-1} \end{bmatrix} Q_L, \tag{12}$$

where μ stands for the matrix of eigenvalues $\{\mu_i\}_{i=1,\dots,n}$. Note that the description provided by Eq. (12) is based on the classification of the eigenvectors into incident and reflected waves (see Ref. [9]). Eqs. (12) and (11) will be used for the estimation of energy velocities.

2.2. Aliasing effects

The practical implementation of the proposed method runs into two main problems. The first one is how to fix the propagation distance, namely d (see Fig. 1). This gives the finite element modeling size whose value cannot be completely arbitrary. The second problem is the pertinent frequency band under consideration.

Along the propagation axis, only one finite element is considered to simplify the formulation. The latter can, however, be easily extended in order to take into account internal degrees of freedom. The chosen finite element must then correctly represent a part of propagating wave along the propagation axis. So, through a kind of Shannon space theorem, pertinent wavelengths or wavenumbers $\{k_j\}_j$ are connected to the

propagation distance through the following simple formula, for the j th propagating branch:

$$\operatorname{Re}\{k_j(\omega)\} < \frac{\pi}{d}. \quad (13)$$

However, it should be mentioned that this value is too far removed from practical applications. Indeed, it is expected that wavenumbers prediction deviations in wavenumber predictions start at around 6 to 10 elements per wavelength often used in FEM calculation. So, errors and deviations are expected to appear around $\operatorname{Re}\{k_j(\omega)\} < (\pi/3d)$ or $\operatorname{Re}\{k_j(\omega)\} < (\pi/5d)$ limit. Hence, large values of d will limit the wavenumber validity domain, and consequently the given frequency band leading to aliasing. Small values of the propagation distance d will lead to two difficulties. The first one is connected to the nature of the employed finite elements. Depending on the cross section shape, d should respect the strain and stress intrinsic limitations. For instance, if thin shells are employed, d must respect the given FE element limitations and their length d should be many times the thickness of the considered elements. The second difficulty is mainly numerical. Small propagation distances will lead to eigenvalues close to unity. Asymptotically, when d tends toward 0, the expression leading to wavenumbers k_j from given propagation constants λ_j , namely:

$$k_j(\omega) = -\frac{\ln(\lambda_j)}{i \times d} \quad (14)$$

becomes singular. Moreover, for weak values of length d , spectral results become very sensitive to numerical errors.

3. Group velocities and energy velocities

3.1. Group velocity expression

The group velocities associated with the guided waves are first discussed. The group velocity of a purely or lightly damped propagating branch j can be readily expressed from the calculated wavenumbers as follows:

$$c_j^g(\omega) = \frac{\partial \omega}{\partial (\operatorname{Re}\{k_j\})}. \quad (15)$$

However the use of this basic formula in the context of multimode guided waves results in a major difficulty. Indeed, the spectral problem solved here provides a set of discrete *unclassified* propagating branches and associated wavenumbers. Moreover, as the frequency increases, the propagating branches can change drastically leading to erroneous evaluation of wavenumbers versus frequency. A classification criterion for wave track purposes and thus, for a safe use of the group velocity expression, is proposed in Ref. [11] as follows: For wave modes j and m defined at frequency ω , such that $\mu_m(\omega) = 1/\mu_j(\omega)$, and for $\Delta\omega$ sufficiently small, find wave mode j at frequency $\omega + \Delta\omega$ such that

$$A_j(\omega) = (\Phi_m(\omega))^T \mathbf{J}_n \Phi_j(\omega + \Delta\omega) \quad (16)$$

is maximized. It should be noticed that wave track index optimization is easier for dissipative cases, compared with conservative ones. So, a very slight damping ratio is introduced as a rule in the wave extraction process to facilitate wave track as well as incident/reflected wave classifications.

Frequency step $\Delta\omega$ must be sufficiently small, meaning that eigenvector Φ_j must vary weakly between frequencies ω and $\omega + \Delta\omega$; In practice, the criterion is verified when eigenvectors $\{\Phi_j\}_j$ are of the same order, which means that they must be normalized in the same way.

The classification criterion coupled to the basic finite difference expression allows numerical evaluation of group velocities for guided multimode wave propagation such that at each frequency step:

$$c_j^g(\omega_n) = \frac{\Delta\omega}{2} \left(\frac{1}{\operatorname{Re}\{k_j(\omega_{n+1})\} - \operatorname{Re}\{k_j(\omega_n)\}} + \frac{1}{\operatorname{Re}\{k_j(\omega_n)\} - \operatorname{Re}\{k_j(\omega_{n-1})\}} \right). \quad (17)$$

The given expression will be employed below as the reference estimation for the energy velocities to be given.

3.2. Energy velocity expression

The calculation of energy velocities is covered in this subsection. It is a well-known physical property that energy velocity is “often” equal to group velocity. The energy velocity is defined rigorously as the ratio between energy flow (active power) and the total stored energy density (kinetic and strain energy densities). The energy flow P evaluated on the left section of any given subsystem of the waveguide can be readily established as follows [4]:

$$P(\omega) = \frac{-i\omega}{4} \begin{pmatrix} \mathbf{q}_L \\ -\mathbf{F}_L \end{pmatrix}^H \mathbf{J} \begin{pmatrix} \mathbf{q}_L \\ -\mathbf{F}_L \end{pmatrix} \tag{18}$$

or equivalently, using modal expansion (11):

$$P(\omega) = \mathbf{Q}_L^H \mathbf{P}^\Phi \mathbf{Q}_L, \tag{19}$$

where \mathbf{P}^Φ stands for the wave energy flow matrix:

$$\mathbf{P}^\Phi = \frac{-i\omega}{4} \begin{bmatrix} \Phi_Q \\ \Phi_F \end{bmatrix}^H \mathbf{J} \begin{bmatrix} \Phi_Q \\ \Phi_F \end{bmatrix}. \tag{20}$$

Here, superscript H stands for the Hermitian (complex conjugate). Expression (19) is a standard description of the active power and is given, for instance, by Miller and von Flotow [12] for a one-dimensional beam like structure. In more recent papers, Langley [4,5] provide some definitions and discussions concerning the properties of the energy flow matrix. The energy velocity associated with the j th propagating branch is then given by

$$c_j^e(\omega) = \frac{P_j}{T_j + U_j}, \tag{21}$$

where P_j is the energy flow contribution of the j th wave to the net energy flowing through the cross section P and where T_j and U_j stand for the kinetic and potential energy densities, respectively. Their sum obviously defines the total energy density. The evaluation of the total energy density stored in the cross section can be achieved in different manners. Indeed, both the stored kinetic energy density and the stored potential energy density should normally be calculated. From the general theory of elasticity under the pure harmonic case, many conclusions can be drawn concerning the wave energetics especially for *unloaded uniform and undamped media*. Under harmonic conditions, it was established that the reactive power divergence is related to the Lagrangian energy density, namely the kinetic energy density minus the potential energy density [13]. For a single propagating wave, the reactive power is zero and thus the kinetic energy density and potential energy density are equal, as are the time-averaged kinetic and strain energies stored in the system. This property will be numerically checked in the context of the multimode wave propagation in the next section. Time-averaged energy quantities are defined as follows:

$$\tilde{T} = \int_{\Omega} T \, d\Omega, \quad \tilde{U} = \int_{\Omega} U \, d\Omega. \tag{22}$$

If the system length d is very small compared to the given wavelengths under interest, the kinetic energy density weakly varies over a typical subsystem length, meaning that the kinetic energy density stored in the left or right cross-section of the subsystem, namely T , can be simply related to the averaged kinetic energy stored by the subsystem, namely \tilde{T} , through the simple first-order developed expression:

$$T = \tilde{T}/d. \tag{23}$$

Thus, observing that in the finite element context, kinetic energy \tilde{T} is written as

$$\tilde{T} = \frac{\omega^2}{4} \begin{bmatrix} \mathbf{q}_L \\ \mathbf{q}_R \end{bmatrix}^H \mathbf{M} \begin{bmatrix} \mathbf{q}_L \\ \mathbf{q}_R \end{bmatrix} \tag{24}$$

leading to

$$T = \frac{\omega^2}{4d} \begin{pmatrix} \mathbf{q}_L \\ \mathbf{q}_R \end{pmatrix}^H \mathbf{M} \begin{pmatrix} \mathbf{q}_L \\ \mathbf{q}_R \end{pmatrix}. \tag{25}$$

Observing that, according to Eqs. (11) and (12)

$$\begin{pmatrix} \mathbf{q}_L \\ \mathbf{q}_R \end{pmatrix} = \left[\begin{array}{c|c} \Phi_q & \mathbf{0} \\ \hline \mathbf{0} & \Phi_q \end{array} \right] \begin{bmatrix} \mathbf{I} & \mathbf{0} \\ \mathbf{0} & \mathbf{I} \\ \mu & \mathbf{0} \\ \mathbf{0} & \mu^{-1} \end{bmatrix} \mathbf{Q}_L \tag{26}$$

leads to

$$T = \frac{\omega^2}{4d} \mathbf{Q}_L^H \mathbf{M}^\Phi \mathbf{Q}_L, \tag{27}$$

where \mathbf{M}^Φ stands for the wave mass matrix, given by

$$\mathbf{M}^\Phi = \begin{bmatrix} \mathbf{I} & \mathbf{0} \\ \mathbf{0} & \mathbf{I} \\ \mu & \mathbf{0} \\ \mathbf{0} & \mu^{-1} \end{bmatrix}^H \left[\begin{array}{c|c} \Phi_q & \mathbf{0} \\ \hline \mathbf{0} & \Phi_q \end{array} \right]^H \mathbf{M} \left[\begin{array}{c|c} \Phi_q & \mathbf{0} \\ \hline \mathbf{0} & \Phi_q \end{array} \right] \begin{bmatrix} \mathbf{I} & \mathbf{0} \\ \mathbf{0} & \mathbf{I} \\ \mu & \mathbf{0} \\ \mathbf{0} & \mu^{-1} \end{bmatrix}. \tag{28}$$

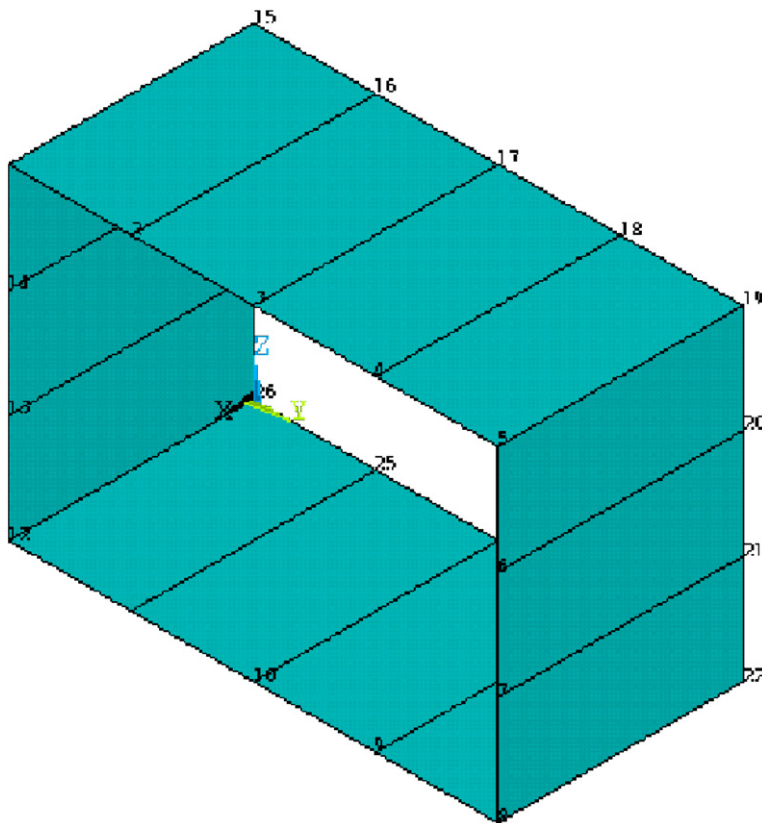


Fig. 2. Thin walled tubular tested structure.

Furthermore, it can be also readily shown that the strain energy density can be expressed as

$$U = \frac{1}{4d} \mathbf{Q}_L^H \mathbf{K}^\Phi \mathbf{Q}_L, \tag{29}$$

where \mathbf{K}^Φ stands for the wave stiffness matrix, given by

$$\mathbf{K}^\Phi = \begin{bmatrix} \mathbf{I} & \mathbf{0} \\ \mathbf{0} & \mathbf{I} \\ \boldsymbol{\mu} & \mathbf{0} \\ \mathbf{0} & \boldsymbol{\mu}^{-1} \end{bmatrix}^H \begin{bmatrix} \Phi_q & \mathbf{0} \\ \mathbf{0} & \Phi_q \end{bmatrix}^H \mathbf{K} \begin{bmatrix} \Phi_q & \mathbf{0} \\ \mathbf{0} & \Phi_q \end{bmatrix} \begin{bmatrix} \mathbf{I} & \mathbf{0} \\ \mathbf{0} & \mathbf{I} \\ \boldsymbol{\mu} & \mathbf{0} \\ \mathbf{0} & \boldsymbol{\mu}^{-1} \end{bmatrix}. \tag{30}$$

The given expression allows computation of the energy densities associated with each propagating branch and provides, according to Eq. (21), a close and analytical expression of the energy velocity as follows:

$$c_j^e = \frac{4d\mathbf{P}_{jj}^\Phi}{\omega^2\mathbf{M}_{jj}^\Phi + \mathbf{K}_{jj}^\Phi}. \tag{31}$$

If the equality between the wave kinetic energy density and the wave strain energy density is considered, then the energy velocity expression becomes:

$$c_j^e = \frac{4d\mathbf{P}_{jj}^\Phi}{2\omega^2\mathbf{M}_{jj}^\Phi}. \tag{32}$$

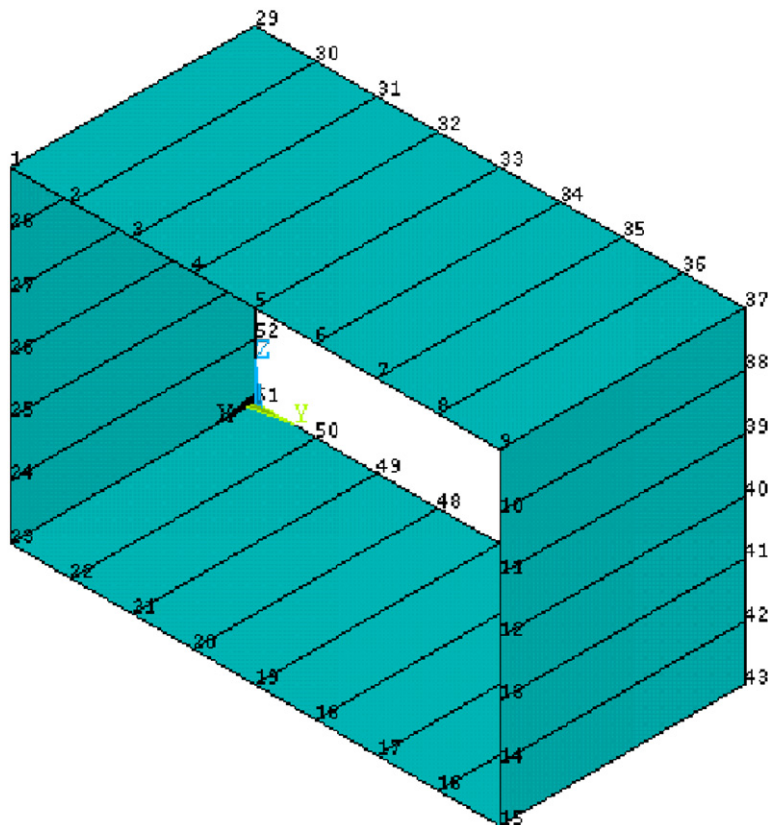


Fig. 3. Thin walled tubular tested structure: refined mesh tested case.

Expressions (31) and (32) represent the explicit analytical expressions of energy velocities in the multimode wave propagation case. In the following section, some numerical experiments are provided for validation purposes.

4. Numerical experiments

The developments established in this study were implemented within a computer code and interfaced with an FEM software. This allows a multimode wave propagation analysis for complex homogeneous and

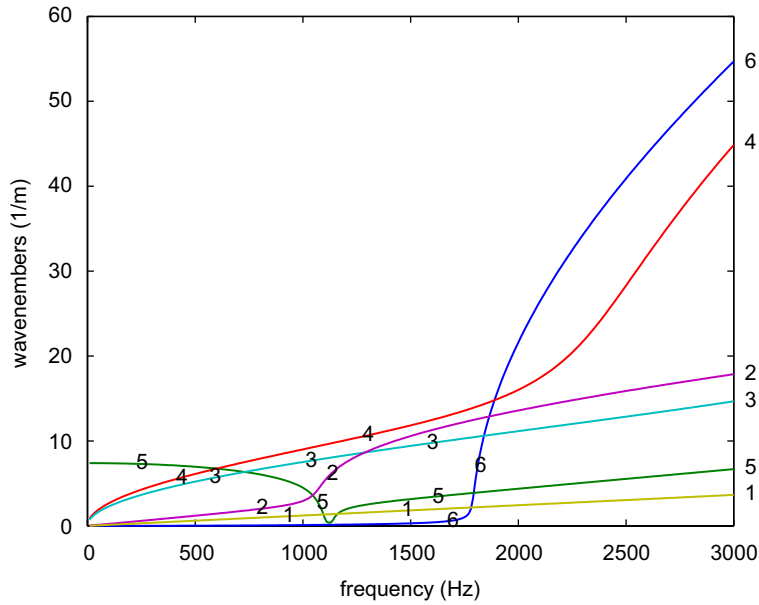


Fig. 4. Tubular structure, dispersion curves ($d = 1$ cm).

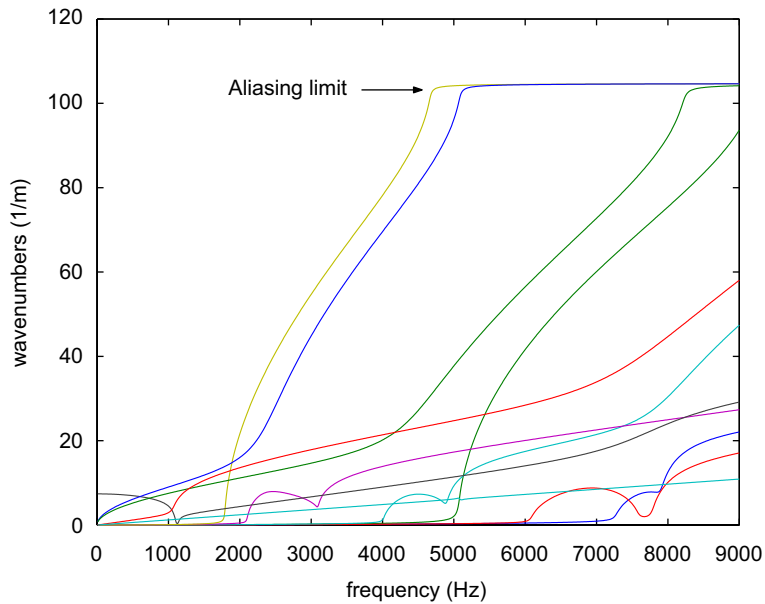


Fig. 5. Tubular structure, dispersion curve ($d = 3$ cm): aliasing effects.

uniform waveguides. For the sake of simplicity, a thin-walled tubular structure is fully tested here. This was also studied in the author’s previous paper [1]. Figs. 2 and 3 show a typical subsystem of the structure. This subsystem is meshed in finite element software using thin shell elements. Fig. 3 shows a refined mesh of the tested subsystem. Here, a thin-wall steel case ($\rho = 7850 \text{ kg/m}^3$, $\nu = 0.3$ and $E = 2.1 \times 10^{11} \text{ Pa}$) is studied

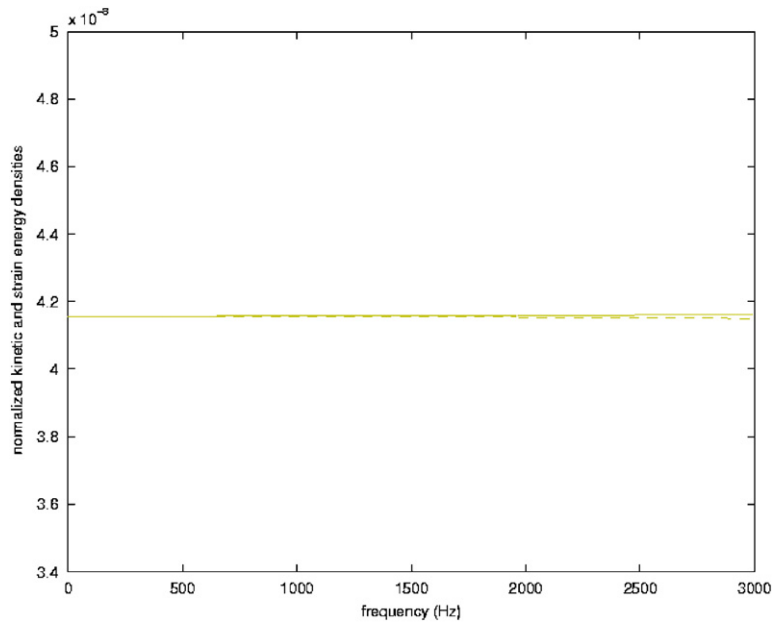


Fig. 6. Kinetic energy density (continuous line) and strain energy density (dashed line) comparison: propagating branch (1)—compression mode.

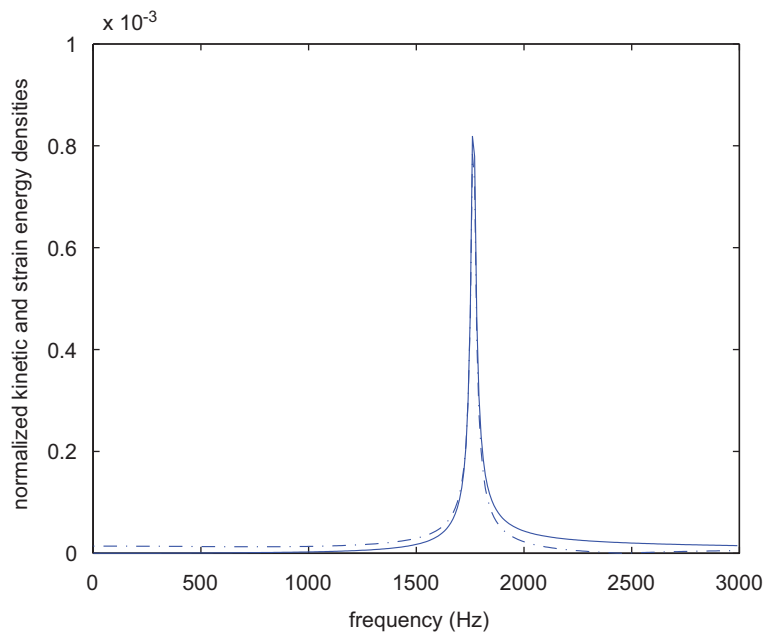


Fig. 7. Kinetic energy density (continuous line) and strain energy density (dashed line) comparison: propagating branch (6)—cross-section mode.

numerically. The tube cross-section is 40 mm by 60 mm and the thickness is 2 mm. For numerical issues and as explained before a very slight damping ratio (of 0.0001 mass proportional) is introduced mainly to facilitate wave track. In view of a parametric analysis, the system length d is chosen equal to 1 and 3 cm, respectively.

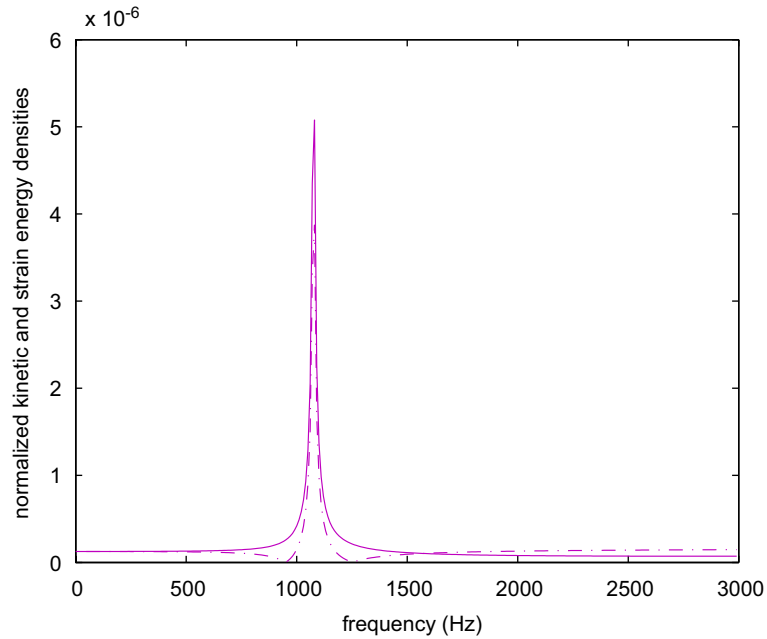


Fig. 8. Kinetic energy density (continuous line) and strain energy density (dashed line) comparison: propagating branch (2)—second extensional mode.

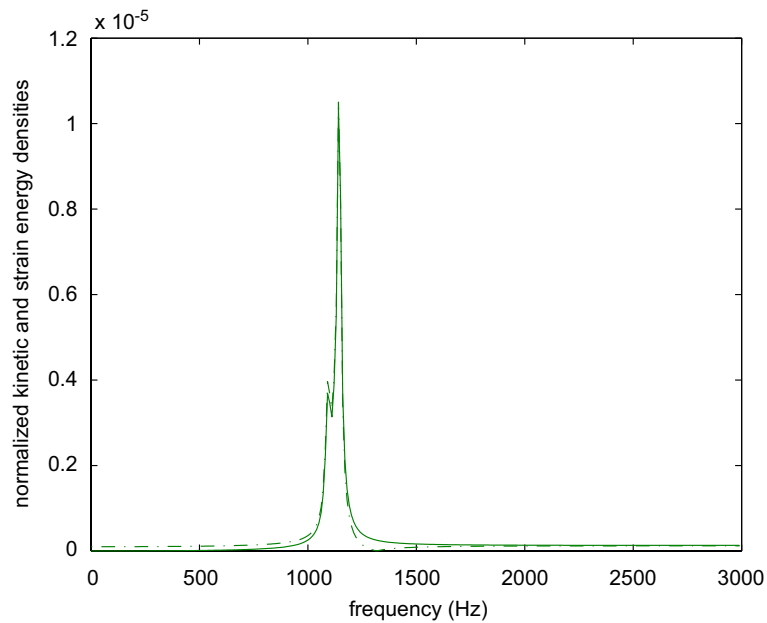


Fig. 9. Kinetic energy density (continuous line) and strain energy density (dashed line) comparison: propagating branch (5)—cross-section mode.

4.1. Aliasing effects

The aim here is to illustrate the aliasing effects discussed above. Fig. 4 shows the dispersion curve of the tubular structure over the frequency band [0, 3000 Hz] in the case of a weak subsystem length ($d = 1$ cm). The propagating branches shown are classified using the wave track index proposed in Eq. (16). For instance, the propagating branch (number 1 in the figure) highlights the low-frequency (LF) compressional and non-dispersive *plane* wave mode. The branches respectively numbered 3, 6 and 5 represent respectively cross-section, extensional and a further cross-section propagating modes, respectively. Fig. 5 shows similar dispersion curves but computed for a large subsystem length, $d = 3$ cm, and in a relatively wide frequency band [0, 9000 Hz]. The figure shows clearly the aliasing effects corresponding to the approximately

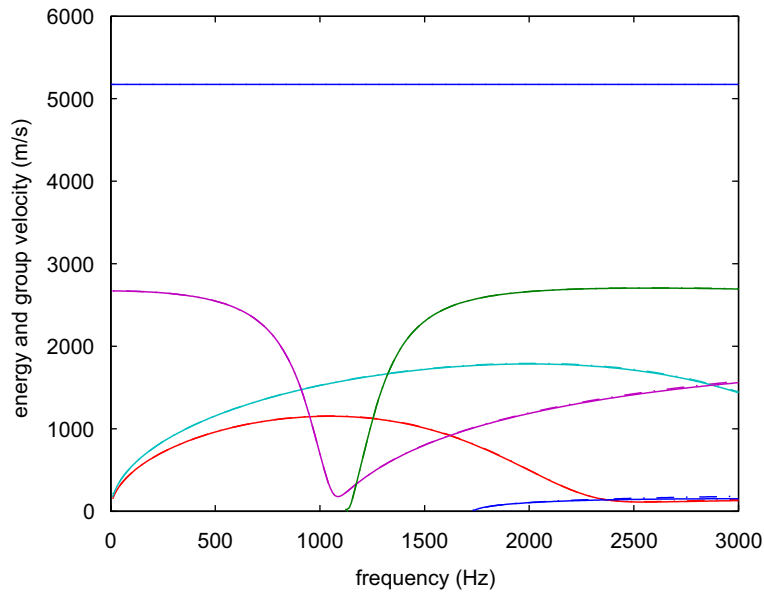


Fig. 10. Group velocities (continuous line) and energy velocities (dashed line) comparisons ($d = 1$ cm).

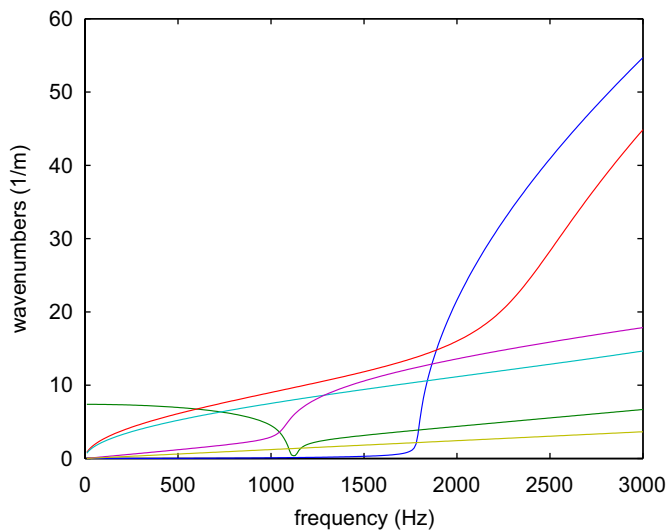


Fig. 11. Dispersion curves, ($d = 3$ cm): aliasing effects suppressed.

33π wavenumber limit (corresponding to $\pi/0.03$) as given in Eq. (13). As shown above, deviations (due to FEM errors) appear at approximately $\pi/3 \times 0.03$ which is the six element per wavelength rule in FEM calculation.

4.2. Energy densities

Some wave kinetic and strain energy densities are also computed. Figs. 6–9 compare wave kinetic energy density, provided by Eq. (27), to the wave strain energy density, provided by Eq. (29). The equality between both quantities seems almost clear. Discrepancies between the strain and kinetic energy densities can be explained by the slight damping introduced in the numerical simulations.

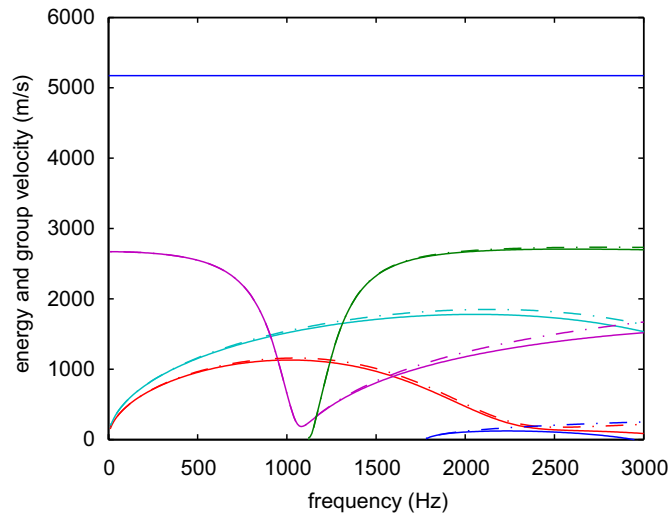


Fig. 12. Group velocities (continuous line) and energy velocities (dashed line) comparisons, ($d = 3$ cm).

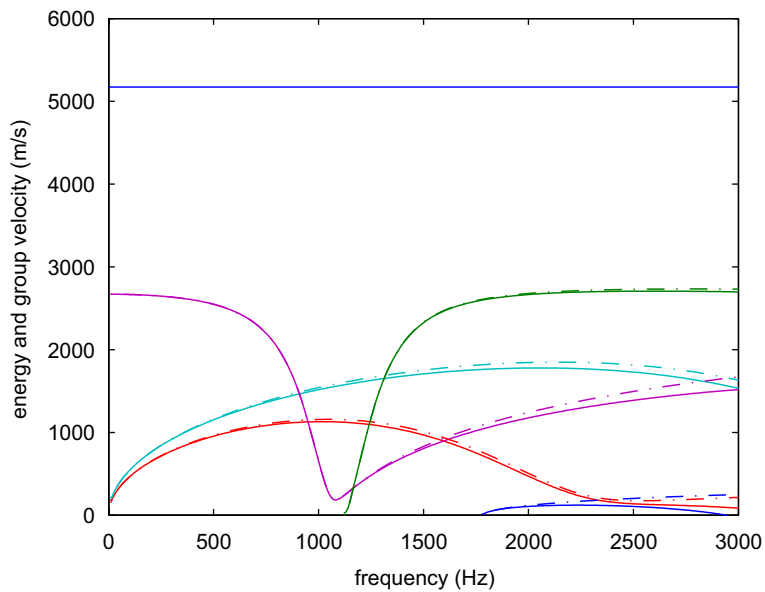


Fig. 13. Group velocities (continuous line) and energy velocities (dashed line) comparisons, ($d = 3$ cm): refined mesh tested case.

4.3. Group and energy velocities comparison: test with a small subsystem length

Here the group velocities and the energy velocities are computed for a small subsystem length ($d = 1$ cm). The group velocities are computed using expression (17), whilst the energy velocities are deduced from expression (32). The comparisons show very good agreements between both definitions and confirm their equality (Fig. 10).

4.4. Group and energy velocities comparison: test with a large subsystem length

In a large system length case ($d = 3$ cm), Fig. 11 shows the dispersion curve extracted without any kind of aliasing. Fig. 12 compares group velocities and energy velocities for the tubular structure given in Fig. 2 and shows some deviations between the two quantities especially at higher frequencies. Fig. 13 confirms these tendencies in the more refined mesh considered in Fig. 3. The energy velocity expression (32) seems to be quite sensitive to the system length.

5. Conclusions

This study aims to complete the author's previous paper [1] addressing the numerical sensitivity of the proposed approach and its post processing for the estimation of group velocities and energy velocities. The main results can be summarized as follows:

- Aliasing effects were discussed. The frequency band versus wavenumbers range was connected to the finite element modeled subsystem for length d . Expression (13) provides a simple criterion to perform the simulation. However, it should be pointed out that the parameter d must also be connected to the nature of employed elements.
- The calculation of guided waves group velocities through a numerical procedure was explained. The main concern here was the criterion of wave track versus frequencies. Expression (16) provides an efficient indicator for that purpose.
- The energetics of multimode guided wave propagation were also discussed. Expression (18) gives the energy flow formula in the wave space, whilst Eqs. (27), (29) provide an estimation of kinetic and strain energy densities. Analytical expressions of energy velocities were provided in expressions (31) and (32). Energy velocities were compared to group velocities, and the sensitivity of energy velocities to the finite element system characteristics was shown.

Further investigations are in progress to enrich the content presented in this study to multi-layer waveguides, to composite structures and to fluid–structure interaction problems.

References

- [1] L. Houillon, M.N. Ichchou, L. Jezequel, Wave motion in thin walled structures, *Journal of Sound and Vibration* 281 (2005) 483–507.
- [2] B. Mace, D. Duhamel, M.J. Brennan, L. Hinke, Finite element prediction of wave motion in structural waveguides, *Journal of Acoustical Society of America* 117 (2005) 2835.
- [3] S. Finnveden, Evaluation of modal density and group velocity by a finite element method, *Journal of Sound and Vibration* 273 (2004) 51–75.
- [4] R.S. Langley, Wave evolution, reflection and transmission along inhomogeneous waveguides, *Journal of Sound and Vibration* 227 (1) (1999) 131–158.
- [5] R.S. Langley, A transfer matrix analysis of the energetics of structural wave motion and harmonic vibration, *Proceeding of the Royal Society of London A* (452) (1996) 1631–1648.
- [6] W.X. Zhong, F.W. Williams, On the direct solution of wave propagation for repetitive structures, *Journal of Sound and Vibration* 181 (3) (1995) 485–501.
- [7] L. Brillouin, *Wave Propagation in Periodic Structures*, McGraw-Hill Publishing Company, New York, 1946.
- [8] A. Bocquillet, M.N. Ichchou, L. Jezequel, Energetics of axisymmetric fluid-filled pipes up to high frequencies, *Journal of Fluids and Structures* 17 (2003) 491–510.

- [9] J.-M. Mencik, M.N. Ichchou, Multi-mode propagation and diffusion in structures through finite elements, *European Journal of Mechanics—A/Solids* 24 (5) (2005) 877–898.
- [10] Y. Yong, Y.K. Lin, Propagation of decaying waves in periodic and piecewise periodic structures of finite length, *Journal of Sound and vibration* 129 (2) (1989) 99–118.
- [11] J.-M. Mencik, M.N. Ichchou, Wave finite elements in guided elastodynamics with internal fluid, *International Journal of Solids and Structures* 44 (7–8) (2007) 2148–2167.
- [12] D.W. Miller, A. von Flotow, A travelling wave approach for power flow in structural networks, *Journal of Sound and Vibration* 128 (1) (1989) 145–162.
- [13] Y. Lase, M.N. Ichchou, L. Jezequel, Energy flow analysis of bars and beams: theoretical formulations, *Journal of Sound and Vibration* 192 (1996) 281–305.